



REAL STRUCTURE OF FERRITIC STEEL AND FERRITE PHASE OF DUPLEX STEEL AFTER COLD-ROLLING

J. Čapek, K. Trojan, J. Němeček, N. Ganev

Department of Solid State Engineering, Faculty of Nuclear Sciences and Physical Engineering,
Czech Technical University in Prague
jiri.capek@fffi.cvut.cz

Keywords: ferritic steel, duplex steel, rolling, texture, fibres

Abstract

The aim of this contribution was to compare the real structure of ferritic steel with ferrite phase of duplex stainless steel after cold-rolling. Preferred orientation was studied as a function of thickness reduction of samples. Moreover, phase analysis were performed for determination of strain-induced or temperature-transformed phases. Type and also strength of determined preferred orientation depending on material and thickness reduction were studied. For analyses, X-ray diffraction was used.

Introduction

Duplex stainless steels exhibit high corrosion resistance in many environments, where the standard austenitic and ferritic steels are used and where their properties significantly exceed single-phase steels. Duplex steels combine advantages of both phases and due to two-phase microstructure, certain properties are better than for high-alloyed single-phase steel, e.g. abrasion resistance [1]. Thereby, smaller amount of material is necessary to manufacture function components. Furthermore, duplex steels are due to austenite phase susceptible to mechanical reinforcement, i.e. local changes in mechanical properties of surface layers.

The importance of the preferred orientation (texture) insists in the anisotropy of most material properties. For this reason, the determination and subsequent interpretation of the texture in material engineering is crucial. Moreover, texture analysis during the thermo-mechanical processing of materials provides information on basic mechanisms including deformation, recrystallization or phase transformation. The properties, which are influenced, are the Young's modulus of elasticity, Poisson number, hardness, strength, ductility, abrasion resistance, magnetic permeability, electrical conductivity etc. So-called plastic anisotropy prefers to use a certain slip plane system during deformation. Therefore, materials with a strong texture are used to produce components for which specific properties are required [2]. Major deformation mechanisms responsible for the formation of ferrite and austenite rolling textures in duplex steels should be the

same as in the single-phase steels. However, their contribution and significance are expected to change [3].

1. Theory

Realising that austenite steel has face centred cubic (fcc) lattice with close-packed structure of atoms, the primary slip system is $\{111\} 110$. The number of slip systems is 12, which is sufficient amount to plastic deformation. However due to formation of stair-rod dislocation with small stacking fault energy, the austenite steels are prone to work-hardening, which can caused mechanical modification and inhomogeneities on the rolled surface [4]. On the contrary, the ferrite crystallizes in a body centred cubic (bcc) lattice. The slip direction in bcc materials is always 111 . Since the bcc lattice is not close-packed structure of atoms, more slip planes engage with the deformation, mostly planes $\{110\}$ and $\{211\}$. From these properties emerges that austenite is plastic and ferrite elastic material. It means that three areas exist during mechanical deformation: elastic area (both phases are elastically deformed), elastic-plastic area (harder ferrite is elastically deformed, but austenite is plastically deformed), and plastic area (both phases are plastically deformed). This deformation of two phases with different properties can significantly change the final texture.

Texture is usually interpreted in the form of orientation distribution function (ODF), i.e. using Euler space. Euler space is defined by three rotations of crystallites $\mathbf{g} =$

$\text{ODF}/f(\mathbf{g})$ determines the bulk density of crystals in the $d\mathbf{g}$ direction. The unit of $f(\mathbf{g})$ is multiple of a random distribution and it is normalized to one, which corresponds to the random orientation of crystals. According to crystal symmetry, the Euler space could be reduced, e.g. for cubic symmetry (), see Fig. 1. Generally, metals and alloys with a bcc lattice tend to form textures with fibre components. These fibres are oriented in the Euler space according to rolling (**RD**), transversal (**TD**), and normal (**ND**) directions. For bcc material, there are six characteristic fibres, see Tab. 1, Figs. 1 and 2 [5]. Most orientations are formed into two characteristic fibres of Euler space. During cold rolling, primarily the 110 and 100 -fibres are created. The 110 -fibre is characterized by crystallographic direction n , which is parallel to rolling direction, e.g. $\{001\} 110$, $\{112\} 110$, $\{111\} 110$, $\{110\} 110$.

Table 1. Typical fibre textures for deformed bcc materials.

Fibre						
Axis of fibre	$110 \parallel \mathbf{RD}$	$111 \parallel \mathbf{ND}$	$100 \parallel \mathbf{RD}$	$110 \parallel \mathbf{ND}$	$110 \parallel \mathbf{TD}$ [7] $100 \parallel \mathbf{ND}$ [8]	Defined by maximal intensity

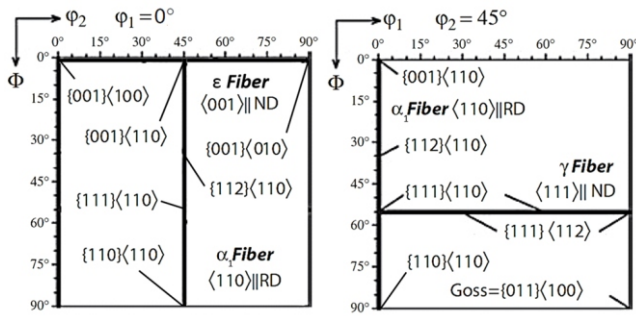


Figure 2. Representation of typical fibre textures of deformed bcc materials.

The α_1 fibre include crystallographic directions with $\{111\}$ planes which are parallel to normal direction, e.g. $\{111\} \parallel 110$, $\{111\} \parallel 112$ [2, 3, 6]. The values of texture components are significantly dependent on the real structure (especially on the grain size and initial texture), chemical and phase composition [3].

2. Experiment

The plate shape samples of size $19 \times 120 \text{ mm}^2$ were made of AISI 420 (ferritic) and AISI 318LN (duplex) type of stainless steel. Before deformation, the samples were annealed in air laboratory furnace for 7 hours at 650°C in order to reduce residual stresses. In the end, the samples were cold-rolled with 0, 10, 20, 30, 40, and 50% reduction of thickness. Therefore, samples made of ferritic and duplex steel are identified by F0–F50 and D0–D50, respectively.

X'Pert PRO MPD diffractometer with $\text{CoK}\alpha$ radiation was used to samples analyses. Texture analysis was performed based on ODF calculation from experimental pole figures which were obtained on three planes $\{110\}/\{220\}$, $\{200\}$, and $\{211\}$ using MTEX software.

3. Results and discussions

3.1 Phase composition

The phase analysis of all samples was performed based on diffraction patterns and the quantitative phase composition was determined using Rietveld method. Only ferrite phase was determined in the single-phase ferritic steel. On the other hand, not only ferrite (α) and austenite (γ) phases, but FeCr (δ) and Cr_{23}C_6 phases were determined in the duplex steel too. The mean weight amount of α , γ , δ , and Cr_{23}C_6 phases were approx. 21 %, 71 %, 5 %, and 3 %, respectively. The calculated amounts of each phase were approximate due to the presence of texture, which increases the error of a phase fracture amount determination in the irradi-

ated volume. The precipitation of undesirable δ and Cr_{23}C_6 phases were caused due to temperature of annealing where δ phase decayed into α and γ phase [9]. On the other hand, due to rolling, the strain-induced martensite could be formed from δ phase. Regarding the presence of the FeCr and Cr_{23}C_6 phases in the duplex steel, the properties, especially strength, are reduced.

3.2 Preferred orientation

In Figs. 3a–c, there are ODF section of ferritic and duplex samples with reduction 0, 30, and 50 %. The ODF sections of samples with 10, 20, and 40% reduction were not attached due to influence ODF changing. Influences of fibre intensities $f(g)$ on the reduction are shown in Figs. 4a–b. Both steels under investigation showed the different starting texture of samples F0 and D0 after thermal treatment, see Figs. 3a. The occurrence of any strong initial texture was not found. Changes of the ferrite texture during cold-rolling of ferritic and duplex steel are shown in Figs. 3b, 3c, and 4.

For ferritic samples F0–F50, the strongest texture components are $\{001\} \parallel 110$ (rotated cubic orientation), $\{112\} \parallel 110$, and $\{111\} \parallel 110$ which are part of the dominant α_1 -fibre. Moreover, the texture components, which are part of α_2 -fibre, are dominant too. Rotated cubic orientation is one of the typical components of ferrite rolling texture. All fibres assume the higher values $f(g)$ for increasing degree of deformation. Fibre α_1 and partly fibre α_2 whose major component is also part of the α_1 -fibre describing the final texture is very inhomogeneous. The ODF sections and fibres depicted in Figs. 3 and 4a are typical for rolling texture of bcc materials.

Despite of ferritic steel, ODFs of α phase of duplex steel do not consist of texture fibre, but only of the particular texture components, see Figs. 3. With increasing rolling reduction the significant increasing of the intensity was observed for the major component $\{001\} \parallel 110$ reaching intensity $f(g) = 18$. For 0–20% rolling reductions, the intensity of texture fibres/components are around value $f(g) = 1.5$, see Fig. 4b. Moreover, after 30% of deformation, intensities of texture components $\{112\} \parallel 110$, $\{111\} \parallel 110$, and $\{111\} \parallel 112$ from the limited α_1 -fibre and α_2 -fibre, respectively, are stronger.

Comparison of ODF sections at Figs. 3 and 4, it is obvious that textures of single-phase ferritic and α phase of two-phase duplex steels are different. Primarily, the reason is different behaviour of particular phases during rolling [10], which follows from specific band-like morphology of

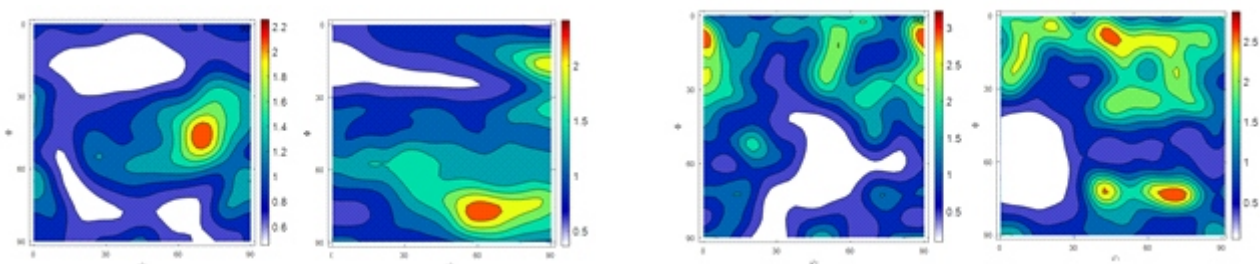


Figure 3a. Sample F0 (two left columns) and D0.

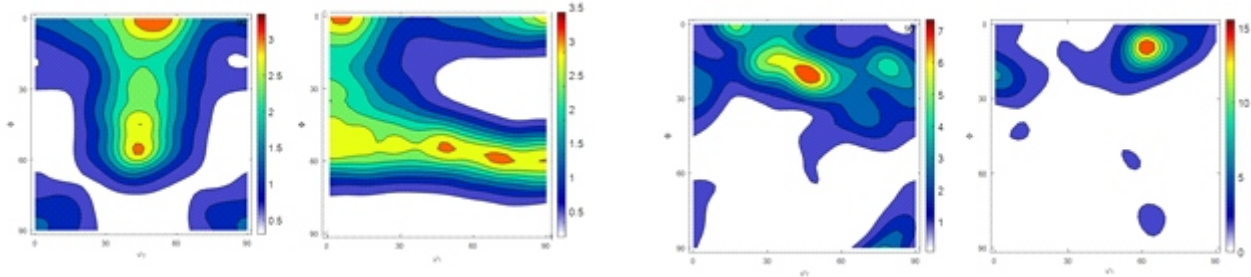


Figure 3b. Sample F30 (two left columns) and D30.

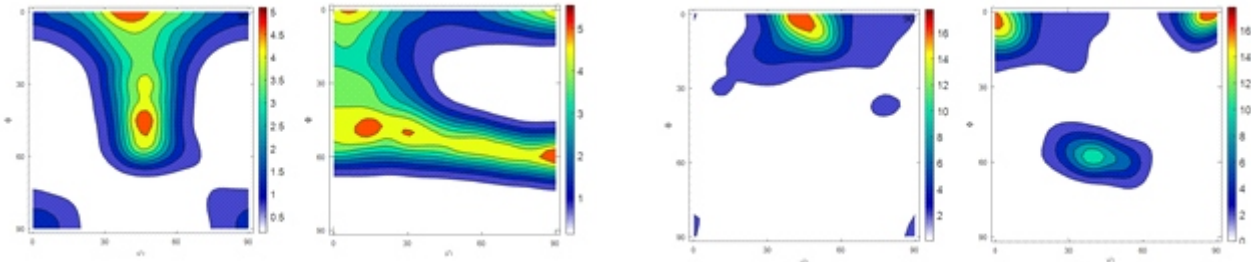


Figure 3c. Sample F50 (two left columns) and D50.

Figure 3. ODF of rolled ferritic (F) and duplex (D) steel in the $\varphi_1 = 0^\circ$ (first and third columns from left) and $\varphi_2 = 45^\circ$ section. The section corresponds with Fig. 2.

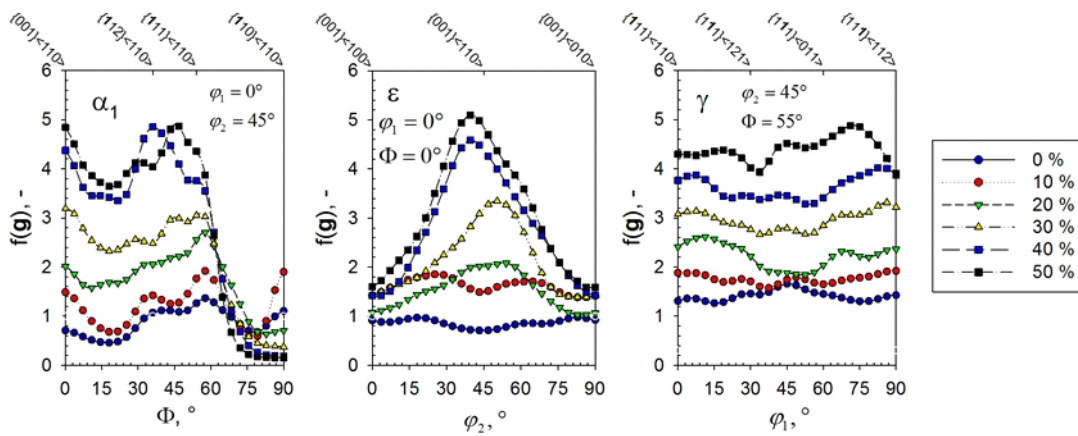


Figure 4a. Values of ODF along individual fibres (φ_1 and φ_2) of ferritic steel.

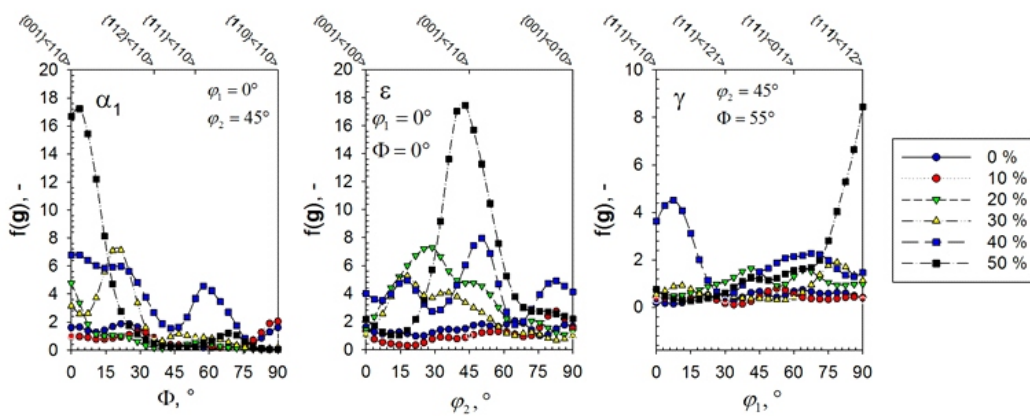


Figure 4b. Values of ODF along individual fibres (φ_1 and φ_2) of ferrite phase of duplex steel..

two-phase structure [3]. Typical rotated cube component for rolling texture of bcc material are presented into both

types of steels. In the case of ferritic steel, the intensity increasing of rotated cube component is gradual. Contrarily,

for α phase of duplex steel, the rotated cube component is sharper.

Because of slip system of bcc materials, fibre-type texture develops in single-phase materials. Therefore, the typical texture components for single-phase steel are $\{001\} 110$, $\{112\} 110$, $\{111\} 110$, and $\{111\} 112$. These components are primarily part of the α_1 and α_2 -fibre. However, in contrast to this, the dominant texture component is only $\{001\} 110$ for α phase of duplex steel. From these results, it is possible to assume that the ferritic phase store the deformation energy. After that, the ferritic grains suddenly rotate to another discrete orientation, i.e. do not form texture with fibre components.

4.. Conclusions

The present study showed:

- Initial texture significantly influences the rolling texture for weak deformations.
- The intensity and development of texture component are different for both types of steels.
- With increasing degree of deformation of ferritic sample, a considerable increasing the texture intensity was observe, from the value $f(g) = 1$ for the starting material to $f(g) = 5$ at 50% of rolling reduction.
- For ferritic sample, there are four main texture components $\{001\} 110$, $\{112\} 110$, $\{111\} 110$, and $\{111\} 112$ which are parts of α_1 and α_2 -fibre.
- For α phase of duplex steel, only rotated cube component $\{001\} 110$ is dominant after 50% deformation.

- The texture for α phase of duplex steel is sharper compared to ferritic sample.

References

1. R. Dakhlaoui, C. Braham, A. Baczmański, *Mater. Sci. Eng.: A*, **70.1**, (2007), 6–17.
2. H. J. Bunge, *Texture Analysis in Materials Science*. London: Butterworth. 1982.
3. J. Ryš, W. Ratuszek, M. Witkowska, *Arch. Metall. Mater.*, **51.3**, (2006), 495–502.
4. K. Kolařík, Z. Pala, N. Ganev, F. Fojtík, *Adv. Mater. Res.*, **996**, (2014), 277–282.
5. S. Suwas, R. K. Ray, *Crystallographic Texture of Materials*. London: Springer-Verlag. 2014.
6. H. Hu, *Texture*, **1.4**, (1974), 233–258.
7. O. Engler, V. Randle, *Introduction to Texture Analysis*. London: Taylor & Francis. 2010.
8. W. Ratuszek, J. Ryš, M. Karnat, *Arch. Metall.*, **45.1**, (2000), 57–70.
9. I. Alvarez-Armas, *Duplex Stainless Steels*. USA: John Wiley & Sons, Inc. 2009.
10. J. Čapek, K. Kolařík, Z. Pitrmuc, L. Beránek, N. Ganev, *Material Structure*, **23.4**, (2016), 362–363.

This work was supported by the Grant Agency of the Czech Technical University in Prague, grant No. SGS16/245/OHK4/3T/14.